Kent Academic Repository

Islam, Jahedul, Meraj, Sheikh Tanzim, Masaoud, Ammar, Mahmud, Md. Apel, Nazir, Amril, Kabir, Muhammad Ashad, Hossain, Md. Moinul and Mumtaz, Farhan (2021) *Opposition-Based Quantum Bat Algorithm to Eliminate Lower-Order Harmonics of Multilevel Inverters.* IEEE Access, 9 . pp. 103610-103626.

Opposition-based Quantum Bat Algorithm to Eliminate Lower-order Harmonics of Multilevel Inverters

Jahedul Islam[1], Sheikh Tanzim Meraj[2], Ammar Masaoud[3], Md. Apel Mahmud[4], Amril Nazir[5], Muhammad Ashad Kabir[6], Md. Moinul Hossain[7], Farhan Mumtaz[2]

[1]Department of Fundamental and Applied Sciences, Universiti Teknologi PETRONAS, Seri Iskandar 32610, Perak Darul Ridzuan, Malaysia
[2]Department of Electrical & Electronic Engineering, Universiti Teknologi PETRONAS, Seri Iskandar 32610, Perak Darul Ridzuan, Malaysia
[3]Electrical Power & Energy Systems Research Lab (EPESRL), School of Engineering, Deakin University, Geelong VIC 3217, Australia
[4]Faculty of Mechanical and Electrical Engineering, Al-Baath University, Homs 97009, Damascus, Syria
[5]Department of Information Systems, Zayed University, Abu Dhabi 144534, United Arab Emirates
[6]School of Computing and Mathematics, Charles Sturt University, Bathurst NSW 2795, Australia
[7]School of Engineering and Digital Arts, University of Kent, Canterbury, Kent, CT2 7NT, UK

Corresponding author: Ammar Masaoud (Email: ammarshz@yahoo.com).

ABSTRACT Selective harmonic elimination (SHE) technique is used in power inverters to eliminate specific lower-order harmonics by determining optimum switching angles that are used to generate Pulse Width Modulation (PWM) signals for multilevel inverter (MLI) switches. Various optimization algorithms have been developed to determine the optimum switching angles. However, these techniques are still trapped in local optima. This study proposes an opposition-based quantum bat algorithm (OQBA) to determine these optimum switching angles. This algorithm is formulated by utilizing habitual characteristics of bats. It has advanced learning ability that can effectively remove lower-order harmonics from the output voltage of MLI. It can eventually increase the quality of the output voltage along with the efficiency of the MLI. The performance of the algorithm is evaluated with three different case studies involving 7, 11, and 17-level three-phase MLIs. The results are verified using both simulation and experimental studies. The results showed substantial improvement and superiority compared to other available algorithms both in terms of the harmonics reduction of harmonics and finding the correct solutions.

INDEX TERMS power electronics, multilevel inverter (MLI), optimization algorithm, pulse width modulation (PWM), selective harmonic elimination (SHE), total harmonic distortions (THD).

I. INTRODUCTION

The operating principle and effective performance of a multilevel inverter (MLI) highly depends on its switching operation. Moreover, the switching operation of an MLI is precisely controlled using a specific pulse width modulation (PWM) technique [1]. The PWM technique makes a power inverter suitable for medium and high voltage industrial applications. The PWM techniques can be classified into sinusoidal PWM (SPWM), space vector PWM (SVPWM), and selective harmonic elimination PWM (SHEPWM). The SHEPWM can be implemented following two steps. In the first step, Fourier analysis will be conducted on the PWM waveform to determine a specific number of switching angles by solving a set of nonlinear transcendental equations. In the second step, these switching angles will be used in

PWM which will set certain lower-order harmonics to zero and will only keep the fundamental at a preset value [2]. The SHEPWM provides significant advantages over other modulation techniques such as improves performance by reducing the ratio between switching frequency and fundamental frequency, increases the voltage gains and bandwidths of MLIs, reduce the requirements of additional filters, prevents the presence of harmonic interference in external line filtering networks, and eliminates the triplen harmonics which can substantially increase the performance and power quality of three-phase systems [1].

A. RELATED WORK
The SHEPWM has been applied in numerous industrial applications, in particular, high-voltage high-power inverters

where power loss is a major issue. However, finding an accurate implementation of the SHEPWM has introduced a lot of challenges. One of the major concerns is the analytical solution for determining the optimum switching angles [3], [4]. In literature, numerous techniques have been proposed such as; Newton-Raphson iterative approach [5]–[7], resultant theory-based approach [8], current reference-based approach [9], Walsh functions [10], gradient method [11], and meta heuristic optimization techniques [12]. In the Newton-Raphson (NR) approach, initial values need to be set. However, there is no established formula to select the initial values making the whole process highly unreliable and complicated. In addition, the optimization performance of NR is very sluggish, and it cannot produce wide range of solutions specially for lower-level MLIs [5]. Walsh functions for the SHEPWM was proposed in [10] to determine the optimum switching angles. It utilizes Walsh transformation matrix to convert transcendental equations into linear equations. Nevertheless, the formulation of the transformation matrix varies for individual problem making it mathematically burdensome. In addition, the characteristics of the nonlinear equations associated with SHEPWM can lead to multiple local-optimum of the objective function, resulting the problem of finding global or near-global optimum solutions.

To address the drawbacks, meta heuristic optimization techniques also known as particle swarm optimization (PSO) are proposed as an evolutionary algorithm for the SHEPWM [13]. The main advantages of PSOs are their learning ability to determine optimum switching angles with high accuracy for a broad range of modulation indices. Therefore, a large number of metaheuristic algorithms, such as whale optimization algorithm (WOA) [14], differential evolution (DE) [15], differential harmony search (DHS) [16], genetic algorithm (GA) [17], improved immune algorithm (IIA) [18], and bacterial foraging (BP) algorithm [19] are utilized to enhance the performance of the SHEPWM.

Although the WOA has a broad range of solutions for a specific benchmark, the solutions could not eliminate the harmonics satisfactorily. DE and DHS have a similar problem whereas, the GA provides a simple mathematical burden-free structure. However, it has the inherent drawbacks of optimal local and slow convergence which can affect the performance of the MLIs. The performance of GAs is highly dependent on the possibility of crossover and mutation. The erroneous selection of input parameters in the GA will reduce its performance and searchability. To improve the performance of the conventional GA, other variants hybrid genetic algorithms and the adaptive real coding GA is proposed to solve the drawbacks of the conventional GA-based SHEPWM [17]. Optimized GA techniques were proposed by integrating an artificial neural network (ANN) [20] [21], where the GA was initially used to optimize the switching angles of the SHEPWM, and then the ANN was used to select the best set of solutions.

However, the results were not satisfactory as this technique was only applicable to high-frequency modulation techniques and they also suffer from the blackbox constraints of neural networks [22], [23]. In the case of the IIA, the final results were highly unsatisfactory as reported in [18]. As a result, this algorithm could not produce any solution and decrease the total harmonic distortions (THD) after the modulation index has reached a certain value. A similar type of outcome can also be observed for the BP algorithm where the intended THDs could not be eliminated using the objective functions.

B. RESEARCH GAP AND MOTIVATIONS

Although the aforementioned techniques provide faster and effective solutions, they suffer from the local optima, slow convergence, and require multi-parameter tuning [17], [20]. Also, few case studies cannot validate the superiority of an algorithm over other algorithms. This is because the performance of these algorithms can widely vary depending on SHEPWM parameters such as the number of voltage levels produced by MLIs, number of targeted harmonics, number of switching angles, and sets of nonlinear equations [4], [15]–[18]. This also demands an algorithm that can be proven superior to other algorithms under various case studies taking different sets of SHEPWM parameters.

A. RESEARCH CONTRIBUTIONS

Quantum-based optimization technology has been applied to a variety of complex engineering applications through parallel quantum mechanisms. For multimodal optimization applications, quantum algorithms are superior to existing metaheuristic algorithms [24]–[27]. The location of each bat in quantum bat algorithm (QBA) relies on the best average position. Besides, incorporating mean best can make the search algorithm jump from the local optima [28], [29]. Therefore, QBA can easily avoid local optimal. Similarly, opposition-based learning (OBL) is integrated with the basic QBA algorithm to improve convergence speed and solution quality. The reason for choosing OBL is that it does not depends on specific algorithm to accelerate the convergence of optimization techniques. To find a better candidate solution, the estimated value and the corresponding opposite estimated value can be closer to the global optimal than the random candidate solutions.

The main contributions of this study can be summarized as below:
1. This article adopts an effective opposition-based quantum bat (OQBA) metaheuristic algorithm to solve the nonlinear SHEPWM problem and to explore search space more effectively. It can overcome most of the problems that exist in other algorithms.
2. Three different case studies are considered to validate the performance of the proposed algorithm.
3. Selective harmonics are eliminated ensuring that two fundamental objectives are satisfied. The first objective

is to ensure that optimized switching angles can eliminate the harmonics satisfying IEEE 519 standard. This standard ensures that the MLI structure along with its control are suitable for industrial applications. The second objective is to have a broad range of solutions that will ensure the flexibility of the MLI or in other words, it can be operated at different modulation indices seemingly.

II. PROPOSED ALGORITHM

The proposed algorithm is the combination of a quantum bat algorithm and opposite-based learning theory. This section gives an overview of the quantum bat algorithm, opposite-based learning and opposition-based quantum bat algorithm.

A. QUANTUM BAT ALGORITHM

Quantum bat algorithm (QBA) is constructed utilizing three habitual characteristics of bats as shown in Fig. 1. The 1st characteristic is known as the echolocation technique which is to sense the distance and measure the difference between their prey (food) as well as background barriers. The 2nd characteristic is to search their prey by varying their wavelength and intensity of sound. Also, the frequency and pace of their emitted pulses can be regulated and scaled to the distance of their prey. The final characteristics can be built by assuming that the intensity of sound can be varied from a minimum constant value (A_{min}) to a large (A_0) value. The velocities (v_i) and positions (x_i) of the bats can be reformed using the following equations:

$$f_i = f_{\min} + (f_{\max} - f_{\min})\alpha \qquad (1)$$

$$v_i^t = v_i^{t-1} + (x_i^t - g^t)f_i \qquad (2)$$

$$x_i^t = x_i^{t-1} + v_i^t \qquad (3)$$

where f_i is the frequency of the pulse, f_{min} is minimum frequency and f_{max} is maximum frequency. α stands for random vector, v_i^t, denote velocity and x_i^t denotes the position, where i is the order of bat and t is the iteration number, and g^t is the global location found by the bats until tth iteration. v_i^{t-1} is the velocity and x_i^{t-1} is the position same bat at (t-1) iteration.

The generation of positions for respective bat from a local random walk is executed when a solution is picked from the present best solutions. The recent position of the bat can be formulated as:

$$x_{new} = x_{old} + \varepsilon A^t \qquad (4)$$

where x_{new} is the new position x_{old} is the old position of bat, ε stands for a random number in the ranges from -1 to 1 and A^t indicates the average intensity of melody of bats while t is the iteration number. A new position of a bat is calculated in OQBA, with the help of (5) and (6):

$$x_{id}^{t+1} = g_d^t \times [1 + j(0,\sigma^2)] \qquad (5)$$
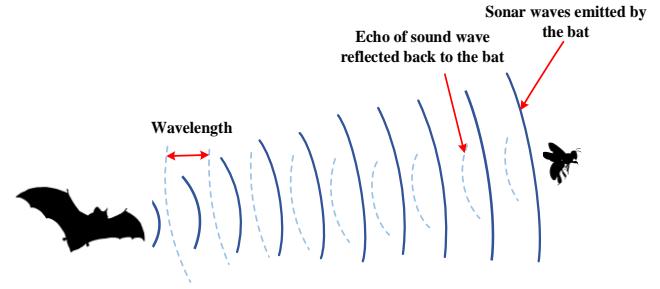
$$\sigma^2 = |A_i^t - A^t| + \varepsilon \qquad (6)$$

FIGURE 1. Search technique for bats.

where, $j(0, \sigma^2)$ symbolizes a Gaussian distribution with mean 0 as well as standard deviation σ^2, x_{id}^{t+1} indicates bat position, and the bat**s** at dimension d help to find current best global location. The integration of ε ensures that the standard deviation always stands positive.

The loudness of sound and pulse rate are presented by A_i and r_i that are upgraded in every iteration by these equations:

$$A_i^{t+1} = \delta A_i^t \qquad (7)$$

$$r_i^{t+1} = r_i^0[1 - exp(-\gamma t)] \qquad (8)$$

where A_i^t and A_i^{t+1} is the loudness of sound for ith bat in t and $t+1$ iteration, respectively, r_i^0 represents the preliminary pulse discharge rate and r_i^{t+1} represents the next pulse discharge rate. Constant δ varies from 0 to 1 and γ is another constant which is greater than zero ($\gamma > 0$).

Apart from the three fundamental characteristics or idealized rules, two more characteristics also have been taken into account in this algorithm. These characteristics can be listed as: (i) the bat population will have several hunting habitats which can be separated from each other rather than depending on one single hunting habitat depending on a suspected selection and, (ii) the bats will have a noteworthy self-adaptive ability that will help them for compensating the complication of doppler effect. The Position of virtual bats with quantum behavior can be described as:

$$x_{id}^t = g_d^t + \beta|mbest_d - x_{id}^t|ln\left(\frac{1}{u}\right), u(0,1) < 0.5 \qquad (9)$$

$$x_{id}^t = g_d^t + \beta|mbest_d - x_{id}^t|ln\left(\frac{1}{u}\right), u(0,1) < 0.5 \qquad (10)$$

where x_{id}^t presents ith bat's position in dimension d at t iteration, β stands for contraction coefficient, u presents a random number, $mbest_d$ is average of all bats position at d dimension.

In the case of the doppler effect the bats needs to initiate its self-adaptive ability and (1), (2) and (3) can be rewritten as follows:

$$f_{id} = \frac{(340 + v_i^{t-1})}{(340 + v_g^{t-1})} \times f_{id} \times \left[1 + C_i \times \frac{(g_d^t - x_{id}^t)}{|g_d^t - x_{id}^t| + \varepsilon}\right] \qquad (11)$$

$$v_{id}^t = (w \times v_{id}^{t-1}) + (g_d^t - x_{id}^t)f_{id} \qquad (12)$$

$$x_{id}^t = x_{id}^{t-1} + v_{id}^t \qquad (13)$$

$$x_{id}^t = x_{id}^{t-1} + v_{id}^t \qquad (13)$$

where f_{id} represents the bat's frequency in order i in dimension d, C_i denotes constant that is positive of ith bat in the range of [0, 1] and v_g^{t-1} presents the global best position's velocity at iteration $t-1$. The implementation procedure of QBA is depicted in Fig. 2.

B. OPPOSITION-BASED LEARNING (OBL)

Opposite-based learning (OBL) is one of Tizhoosh's important methods for optimizing heuristic optimization [30] to increase the convergence speed. To enforce OBL efficiently, the opposite and existing generations of the same age must be compared to find a better solution to a given problem. To increase the convergence speed, the OBL idea has been used successfully in numerous metaheuristic methods [31], [32]. To understand the OBL, the log definition can be described.

Let $N(N \in [x, y])$ be real number. The reverse is N^0 known as:

$$N^0 = x + y \qquad (14)$$

The definition can be generalized as follows for d-dimensional search spaces:
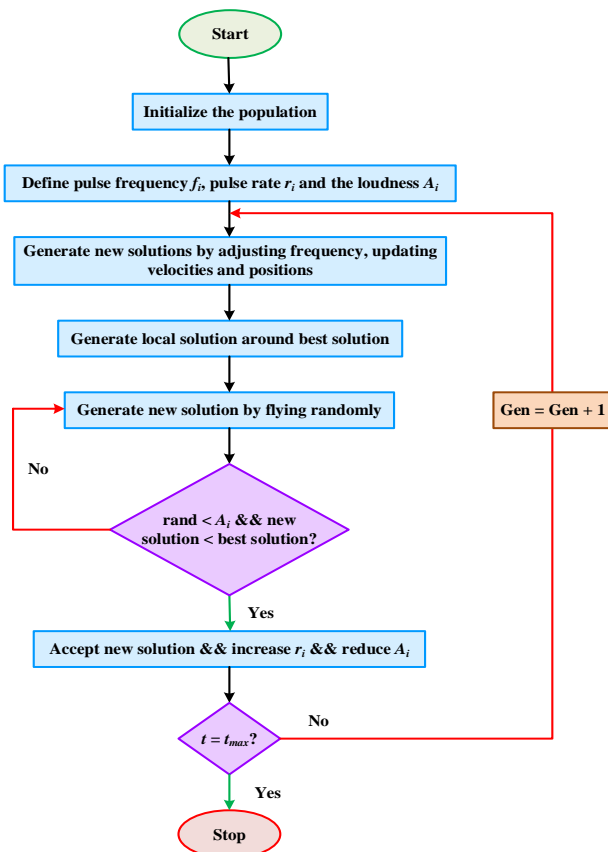

FIGURE 2. The implementation procedure of QBA.

$$N_i^0 = x_i + y_i - N_i \qquad (15)$$

where $(N_1 N_2, \dots N_d)$ is the search space in d-dimensional and $(N_i \in [x_i, y_i]); \ i = \{1, 2.3 \dots d\}$.

The OBL definition is used in each iteration of the initialization process and the use of the generated jumping rate (J_r) in Opposite-based learning (OBL). The following steps demonstrate the different steps for OBL.

Step 1: Randomly initialize people within the operational range in the population.

Step 2: Build the crowd opposite.

for j = 1: size of population

for i = 1: Number of variables power

$$N_{j,i}^0 = x_i + y_i - N_{j,i}$$

end for

end for

Step 3: Sort from highest to lowest the existing population and the relative population

Step 4: Select from the present and relative populations the optimum number of solutions based on the total scale.

Stage 5: Use the recommended optimization technologies to change the control variable for a particular issue.

Step 6: Use the jumping rate to create the opposite population to the current population.

for j = 1: size of population

    for i = 1: Number of variables

        if jumping rate >rand

        opposition(i,j) = min(j)+max(j)-pop(i,j)

        else

        opposition(i,j)=pop(i,j)

        end if

    end for

end for

Step 7: Filter from the best to worst whole (*pop*) and opposite population (*opposition*) and select the best solutions from the whole and family populations

Step 8: If the end condition is fulfilled, interrupt the iteration. Continue to stage 5 of the next generation otherwise.

B. OPPOSITION-BASED QUANTUM BAT ALGORITHM (OQBA)

In this study, OBL and QBA is incorporated. The current populations update position based on QBA technique and the opposite populations are generated from the current

population. After that fitness values of the positions are calculated. This process will iterate until stopping criteria are meet. The pseudocode of the proposed technique is given below:

Pseudocode: Opposition-based Quantum Bat Algorithm

Initialize probability of habitat selection (P), inertia weight (w), compensation rates for Doppler Effect in echoes (C), contraction/expansion coefficient (β), the frequency of updating the loudness and emission pulse rate (G), the number of individuals (N) contained by the population and, initialize the opposite points,

 while (iteration< t_max)

if (rand)<0.5

generate new solutions using (9)

else

generate new solutions using (10)

end if

if (rand(0,1)>r_i)

using equation (4) generate a local solution around the selected best solution

end if

*evaluate the objective function *

using jumping rate, the opposite population are generated from the current population.

evaluate the objective function value of each opposite individual.

update solutions, the loudness, and emission pulse rate using (7) and (8)

rank the solutions and select the first N number of populations

find g^t

if g^t does not improve in G time step.

re-initialize the loudness A_i and set temporary pulse rates r_i [0.85-0.9]

end if

t=t+1;

end while

III. DETERMINATION OF OPTIMUM SWITCHING ANGLES

The schematic diagram of a modular three-phase cascaded H-bridge multilevel inverter (CHBMLI) is shown in Fig. 3. The mathematical expressions of the CHBMLI for the modularity in terms of number of cells (*c*) can be expressed as:

Number of voltage levels, $N_L = 2c + 1$ (16)

Number of switches, $N_S = 4c$ (17)

Maximum voltage, $N_{L\_max} = c$ (18)

Using (16)-(18), 3 three-phase CHBMLIs are developed in this manuscript which can generate 7-level, 11-level and 17-level output voltage. These three case studies will confirm the accurate implementation of the proposed OQBA
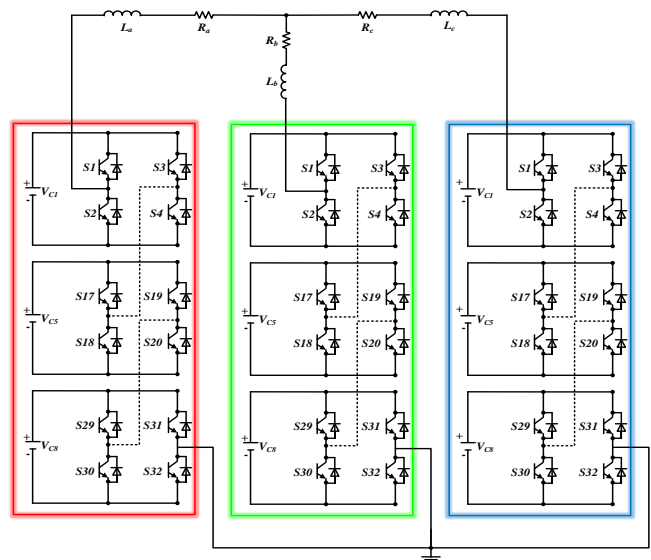

FIGURE 3. A three-phase modular CHB MLI.

As mentioned earlier, the SHEPWM is generally utilized to regulate the fundamental and exterminate preset harmonic components from the output voltage of a single-phase MLI. The voltage waveform of an MLI is usually a bipolar/unipolar rectangular signal which closely resembles a staircase. The fundamental output voltage of an N_{Level} MLI is depicted in Fig. 4. It can be observed that in each edge of each rectangular wave or voltage level, there is one switching angle that is predefined. The optimization of these switching angles ais the key in eliminating specific harmonics from the staircase voltage waveform of the MLI. For a CHBMLI having the ability to produce N_L voltage levels output voltage, the number of switching angles (*S*) can be verified by:

$$S = c = \frac{N_L - 1}{2} \quad (19)$$

Generally, the Fourier series of the output voltage (*v*) of a single-phase MLI is given by:

$$v(t) = x_0 + \sum_{r=1}^{\infty} x_r \cos(r\omega t) + y_r \sin(r\omega t) \quad (20)$$

$$x_r = \frac{2}{T} \int_0^T v(t) \cos(r\omega t)\, dt \quad (21)$$

$$y_r = \frac{2}{T} \int_0^T v(t) \sin(r\omega t)\, dt \quad (22)$$

where, *r* represents the order of the harmonics, x_r denotes even harmonics, y_r denotes odd harmonics, *ω* depicts angular frequency, *t* is the sample time and *T* is the period. Since a conventional CHBMLI has an odd number of voltage levels in a quarter-wave symmetry, only (22) is valid [1]. In other
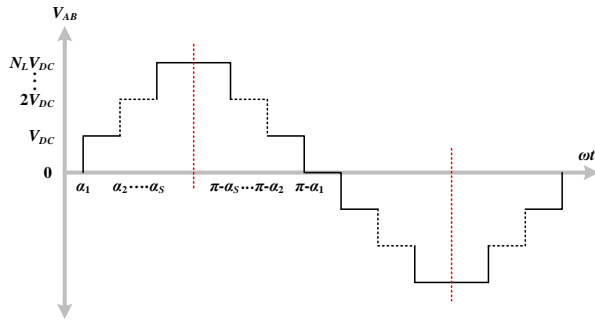
FIGURE 4. Staircase output voltage waveform of N_{Level} CHB MLI.

words, only the sine components of the odd harmonics (y_1, y_3, y_5,......y_n) will exist in the output voltage. Mathematically, it can be expressed as:

$$y_r = \frac{4}{\pi} \int_0^{\frac{\pi}{2}} v(t) \sin(r\omega t) \, d\omega t \qquad (23)$$

In this study, S is determined to be 3, 5, and 8 for the 7, 11, and 17-level CHBMLIs, respectively according to (17). Therefore, for 7, 11, and 17-level CHBMLIs the number of harmonics that can be eliminated is 2, 4, and 7, respectively. The information regarding the three case studies that are selected for this manuscript is demonstrated in Table I.

By observing Fig. 4, it can be stated that the voltage waveforms have odd quarter cycle symmetry. Thus, the output voltage waveforms of the CHBMLIs can be expressed for the Fourier coefficient y_r, the number of switching angles of each voltage waveform S, and the order of the predefined harmonics h.

For 7-level CHBMLI, the set of nonlinear equations can be obtained by:

$$y_1 = \frac{4V_{DC}}{\pi} [\cos(\alpha_1) + \cos(\alpha_2) + \cos(\alpha_3)] = m$$

$$y_5 = \frac{4V_{DC}}{5\pi} [\cos(5\alpha_1) + \cos(5\alpha_2) + \cos(5\alpha_3)] = 0$$

$$y_7 = \frac{4V_{DC}}{7\pi} [\cos(7\alpha_1) + \cos(7\alpha_2) + \cos(7\alpha_3)] = 0 \qquad (24)$$

Similarly, for 11-level CHBMLI:

$$y_1 = \frac{4V_{DC}}{\pi} [\cos(\alpha_1) + \cos(\alpha_2) + \ldots + \cos(\alpha_5)] = m$$

$$y_5 = \frac{4V_{DC}}{5\pi} [\cos(5\alpha_1) + \cos(5\alpha_2) + \ldots + \cos(5\alpha_5)] = 0$$

$$y_7 = \frac{4V_{DC}}{7\pi} [\cos(7\alpha_1) + \cos(7\alpha_2) + \ldots + \cos(7\alpha_5)] = 0$$

$$y_{11} = \frac{4V_{DC}}{11\pi} [\cos(11\alpha_1) + \cos(11\alpha_2) + \ldots + \cos(11\alpha_5)] = 0$$

$$y_{13} = \frac{4V_{DC}}{13\pi} [\cos(13\alpha_1) + \cos(13\alpha_2) + \ldots + \cos(13\alpha_5)] = 0 \qquad (25)$$

TABLE I
OQBA BASED SHEPWM PARAMETERS FOR THE CASE STUDIES

Parameters	Case 1	Case 2	Case 3
No. of voltage levels (N_L)	7	11	17
Maximum voltage (N_{Lmax})	$3V_{DC}$	$5V_{DC}$	$8V_{DC}$
No. of switching angles (S)	3	5	8
No. of predefined harmonics (h)	2	4	7
Order of eliminated harmonics (r)	5,7	5,7,11,13	5,7,11,13,17, 19, 23
Maximum iteration (t_{max})		500	
Number of swarms (i)		25	
Initial loudness (A_i)		2	
OQBA constant gamma (γ)		0.9	
OQBA constant delta (δ)		0.99	
Contraction coefficient (β)		2	
Initial pulse discharge rate (r_i)		0	
Maximum inertia weight (w_{max})		0.9	
Minimum inertia weight (w_{min})		0.5	
Maximum frequency (f_{max})		1.5	
Minimum frequency (f_{min})		0	
Global location (g)		10	
Maximum compensation (C_{max})		1	
Minimum compensation (C_{min})		0.9	

Finally, for 17-level CHBMLI:

$$y_1 = \frac{4V_{DC}}{\pi} [\cos(\alpha_1) + \cos(\alpha_2) + \ldots + \cos(\alpha_8)] = m$$

$$y_5 = \frac{4V_{DC}}{5\pi} [\cos(5\alpha_1) + \cos(5\alpha_2) + \ldots + \cos(5\alpha_8)] = 0$$

.
.
.
.

$$y_{19} = \frac{4V_{DC}}{23\pi} [\cos(23\alpha_1) + \cos(23\alpha_2) + \ldots + \cos(23\alpha_8)] = 0 \quad (26)$$

where V_{DC} symbolizes each level of CHBMLI's output voltage and m represents the modulation index. It is worth noting that the 1st switching angle α_1 is used in (24)-(26) to control the fundamental component of the voltage output while all other switching angles (α_2, α_3, ..., α_S) are used to eliminate the predefined harmonic components.

The switching angles for the case studies are solved by utilizing an objective function. OQBA algorithm finds the optimal solution using this objective function. In general, the function can be defined by:

$$F(\alpha_1 \ldots \alpha_S) = \left[\left(\sum_{i=1}^{S} \cos(\alpha_i) - S \times m \right)^2 + \left(\frac{4}{5\pi} \sum_{i=1}^{S} \cos(5\alpha_i) \right)^2 \ldots \right.$$
$$\left. + \left(\frac{4}{h\pi} \sum_{i=1}^{S} \cos(h\alpha_i) \right)^2 \right] \qquad (27)$$

Here, F represents the fitness value. The objective function is subjected to a boundary condition depending on which the optimum switching angles are selected. The boundary condition is:

$$0 \le \alpha_1 \le \alpha_2 \le \ldots \le \alpha_S \le \frac{\pi}{2} \qquad (28)$$

The switching angles determined by (27) using OQBA is

checked whether it satisfies (28) or not. If they do not satisfy (28), they are considered as garbage values and are not used. In each trial for each case study, a specific amount of iteration and swarms are selected to conduct OQBA based SHEPWM. These values are demonstrated in Table I. In each iteration, the switching angle variables are updated using OQBA along with the fitness value. The algorithm considered the value of m from 0.1 to 1 with 0.001 interval. For a certain value of m, the algorithm finds the minimum fitness value.

IV. NUMERICAL SIMULATIONS

A. CASE STUDY 1: 7-LEVEL CHB MLI

The solutions of this case study are determined for a 7-level CHB MLI. The necessary parameters required for the optimization are demonstrated in Table I. It is worth noting that the OQBA possesses the ability to evade local optima and thus for each iteration, it can generate more than one result. The computed switching angles are plotted in Fig. 5 under different modulation indices. The OQBA based optimization is carried out using MATLAB Simulink. To conduct the simulation, each CHB cell is connected with a DC source of 50V. Thus, in this case, the CHB MLI can generate a maximum of 150V output voltage. The optimized switching angles for each modulation index and the generated THD of the output voltage are shown in Table II. The voltage THD can be calculated as follows:

$$THD(\%) = \frac{\sqrt{\sum_r^h V_{r\_rms}^2}}{V_{1\_rms}} \quad (29)$$

where, $V_{r\_rms}^2$ is the RMS voltage of the rth harmonic and V_{1_rms} is the fundamental RMS voltage. It can be noticed from Table II that under all modulation indices the THD has reduced because of eliminating 5th and 7th order harmonics from the output voltage. Furthermore, because of implementing a balanced three-phase system, the triplen harmonics (3rd, 9th, 15th....) from the line voltage are also removed which has also contributed towards the reduction of
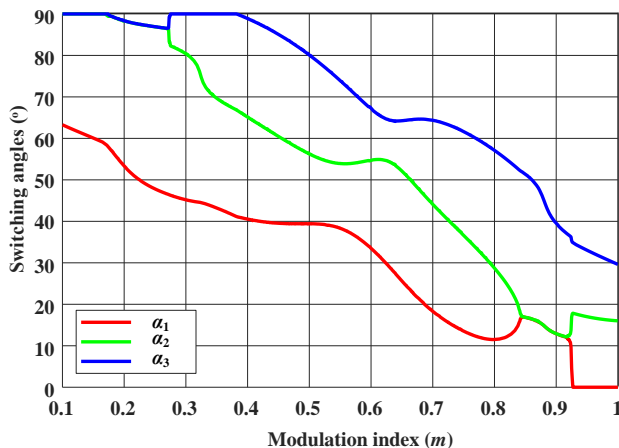

FIGURE 5. Optimum switching angles under different modulation indices for 7-level CHB MLI.

TABLE II
THD Calculation Using OQBA for Case Study 1

Modulation index (m)	Switching Angles (°)			THD (%)
	α_1	α_2	α_3	
0.1	60.33	90	90	40.12
0.2	47.88	86.57	87.29	30.45
0.3	43.27	79.77	90	17.76
0.4	39.55	60.57	85.15	13.11
0.5	38.38	53.94	74.07	9.74
0.6	25.79	52.26	64.24	7.68
0.7	13.67	36.91	61.72	6.41
0.8	11.50	28.89	57.21	5.64
0.9	12.90	13.05	39.66	5.29
1	4.46	16.40	34.33	5.08

the THD [5]. It should be mentioned that in a voltage source inverter, the dominant low-order harmonic are 3rd, 5th, 7th, and 9th [2]. Furthermore, for all the case studies the THD is calculated by taking 40 lower order harmonics into account.

Observing Table II, it is noted that only for the value of m ranging from 0.6 to 1, the THD has followed IEEE 519 standard (i.e. THD ≤ 8%) [33]. In addition, for m = 0.1 and m = 0.2, the switching angles determined by OQBA could not eliminate the targeted harmonics. For the lower modulation indices, the OQBA could not generate accurate switching angles since it required some initial conditions to be met to determine the minimum fitness value and the global best solutions. This issue can be resolved by increasing the number of iteration or increasing the number of switching angles. The first solution is not considered in this study since it can be highly time consuming to execute the proposed algorithm. The second solution is validated in the following case studies which comprises of 5 and 8 switching angles, respectively.

The simulated output voltages and harmonic spectrums of the line voltages of the 7-level CHB MLI are shown in Fig. 6 under 2 different modulation indices. It can be observed from the output voltages' harmonic spectrums that in both instances, the OQBA based SHEPWM eliminated the 5th and 7th order harmonics effectively while the peak voltage increased from 214.7 V to 306.7 V. In addition, the triplen harmonics are also removed from the line voltage. As a result, the overall THD has decreased.

B. CASE STUDY 2: 11-LEVEL CHB MLI

In this case study, OQBA based SHEPWM is executed for an 11-level CHB MLI. Since, the number of voltage levels is increased in this case compared to the previous case, the effectiveness of the proposed optimization algorithm can be further realized. The switching angles computed using OQBA for this case study are plotted in Fig. 7 under different modulation indices while generated THD of the output voltage are shown in Table III. It can be observed that the performance of the OQBA in this case study is more effective and improved. The generated THD has followed IEEE 519 standard under nearly all modulation indices except for 0.1 and 0.2.
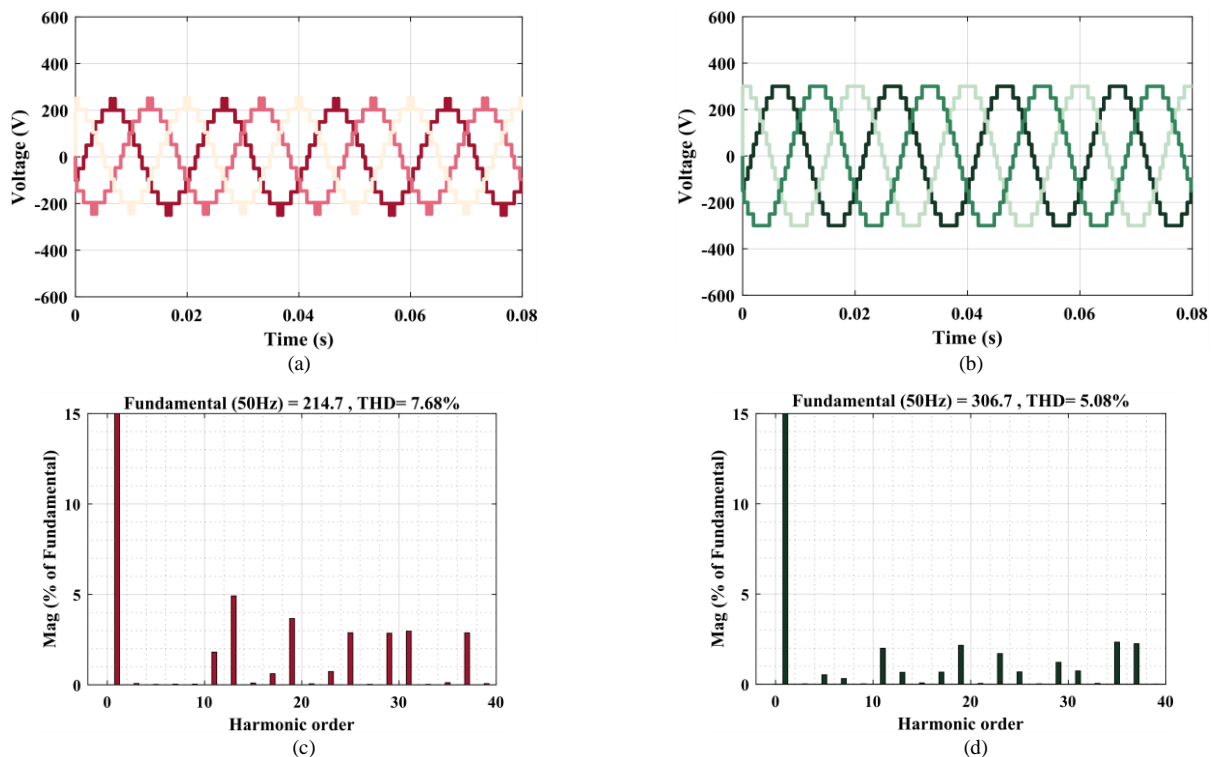
FIGURE 6. Simulation results of three-phase 7-level CHB MLI: (a) line voltages at *m* = 0.6, (b) line voltages at *m* = 1, (c) harmonic spectrum of line voltage *ab* at *m* = 0.6, (d) harmonic spectrum of line voltage *ab* at *m* = 1.
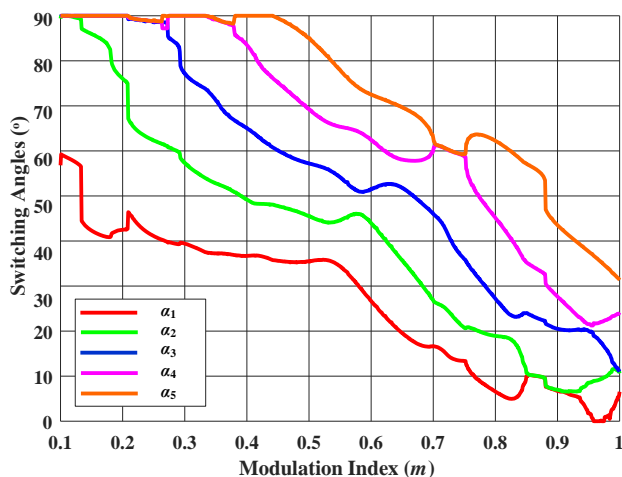

FIGURE 7. Optimum switching angles under different modulation indices for 11-level CHB MLI.

TABLE III
THD CALCULATION USING OQBA FOR CASE STUDY 2

Modulation index (*m*)	Switching Angles (°)					THD (%)
	α_1	α_2	α_3	α_4	α_5	
0.1	42.82	86.49	89.86	89.98	90	27.03
0.2	41.45	62.58	87.64	88.88	89.97	15.37
0.3	36.26	52.85	71.44	88.72	89.80	7.90
0.4	36.71	49.22	65.11	83.66	90	6.47
0.5	35.51	45.55	57.24	69.32	85.04	5.97
0.6	26.82	44.10	51.45	62.52	72.56	5.35
0.7	8.24	28.67	41.30	53.45	73.39	4.62
0.8	6.67	18.96	27.38	45.33	62.33	4.05
0.9	2.23	9.75	19.65	26.87	42.42	2.86
1	3.63	9.53	20.07	28.03	43.60	2.70

C. CASE STUDY 3: 17-LEVEL CHB MLI

This case study comprises the simulation results of OQBA based SHEPWM for a 17-level CHB MLI. A total of 8 switching angles are optimized using OQBA and 7 lower-order harmonics are eliminated. The optimized 8 switching angles under the modulation index ranging from 0.1 to 1 are depicted in Fig. 9. Utilizing the 8 DC sources each generating 50 V, the 17-level CHB MLI can generate 400 V output voltage. The generated THD of the line voltage from the 17-level MLI is shown in Table IV. It can be observed from Table IV that increasing the number of switching variables have improved the performance of the OQBA compared to the previous two case studies. Since 7 lower-order harmonics are removed effectively and the number of voltage levels is increased, 9 out of 10 results of this case study have followed IEEE 519 standards. The simulation results of this case study are shown in Fig. 10

The output voltages of the 11-level CHB MLI are shown in Fig. 8 including the harmonic spectrums of the output voltages under 3 different modulation indices. Utilizing 50V DC source of each CHB cell, the 11-level MLI can generate 250V of the output voltage. Observing Fig. 8, it can be confirmed that the OQBA based SHEPWM has successfully eliminated 5th, 7th, 11th, and 13th order harmonics. Thus, the overall THD in this case study has drastically reduced like the previous case study. In fact, it can be observed that for higher-level output voltage, the performance of the proposed optimization algorithm is comparatively more effective and efficient.
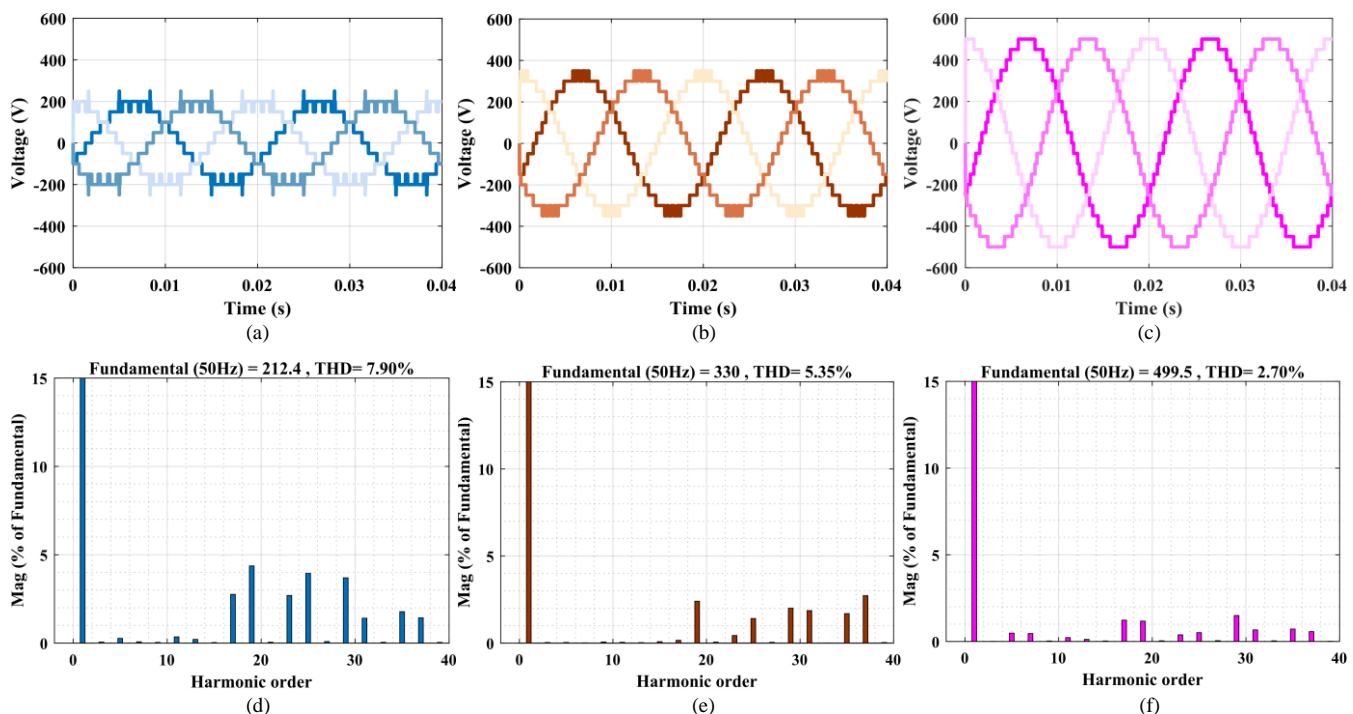
FIGURE 8. Simulation results of three-phase 11-level CHB MLI: (a) line voltages at *m* = 0.3, (b) line voltages at *m* = 0.6, (c) line voltages at *m* = 1, (d) THD of line voltage *ab* at *m* = 0.3, (e) THD of line voltage *ab* at *m* = 0.6, and (f) THD of line voltage *ab* at *m* = 1.
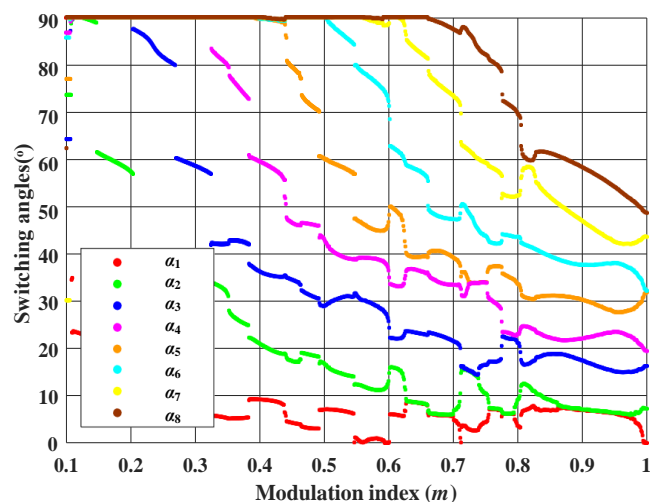

FIGURE 9. Optimum switching angles under different modulation indices for 17-level CHB MLI.

V. COMPARATIVE ANALYSIS

The advantageous and predominant characteristics of the proposed optimization algorithms are validated in this section by comparing it with other algorithms that have already been applied in SHEWPWM. The comparative analysis is conducted considering two major targets: the calculated THD must follow IEEE 519 standards and algorithms must be able to find a wide range of solutions. The proposed algorithm is compared with five other recently proposed algorithms which are named as PSO [13], WOA

TABLE IV
THD CALCULATION USING OQBA FOR CASE STUDY 3

Modulation index (*m*)	Switching Angles (°)								THD (%)
	α_1	α_2	α_3	α_4	α_5	α_6	α_7	α_8	
0.1	38.71	61.97	88.54	89.99	90	90	90	90	14.37
0.2	36.71	49.65	72.35	88.47	89.91	89.91	89.98	90	7.95
0.3	35.14	43.74	53.69	65.15	77.50	89.41	89.60	89.78	6.67
0.4	33.45	40.74	48.30	56.51	64.33	74.34	85.93	90	5.87
0.5	21	33	44.90	51.25	57.64	64.70	72.10	89.34	4.95
0.6	10.96	26.01	36.63	42.31	51.87	59.40	64.31	78.01	4.20
0.7	4.09	14.79	23.38	30.07	41.59	49.12	58.85	70.79	3.60
0.8	6.54	6.72	15.88	20.09	26.55	34.89	46.66	60.20	2.03
0.9	3.51	5.11	9.44	16.28	16.56	25.49	29.92	39.68	1.64
1	2.91	4.91	9.82	14.93	15.76	23.20	26.69	35.22	1.43

[14], DHS [16], GA [17], and IIA [18]. To justify the comparison, the same parameters such as number of iterations, number of search agents are considered for all the algorithms.

It can be observed from Table V that for the 1st case study, most of the algorithms struggled to find global best solutions under all modulation indices. PSO and DE could not find solutions at *m* > 0.5 whereas, WOA performed the worst and could not find solution when *m* > 0.3. None of these three algorithms could generate a single result that has followed IEEE 519 standard. Both PSO and DE requires high number of optimizable variables or iterations to execute SHEPWM properly as reported in [34] and [35], respectively. WOA also performed poorly since this algorithm was developed using the fundamentals of the PSO algorithm and they are highly similar in nature. The results reported in [14] using
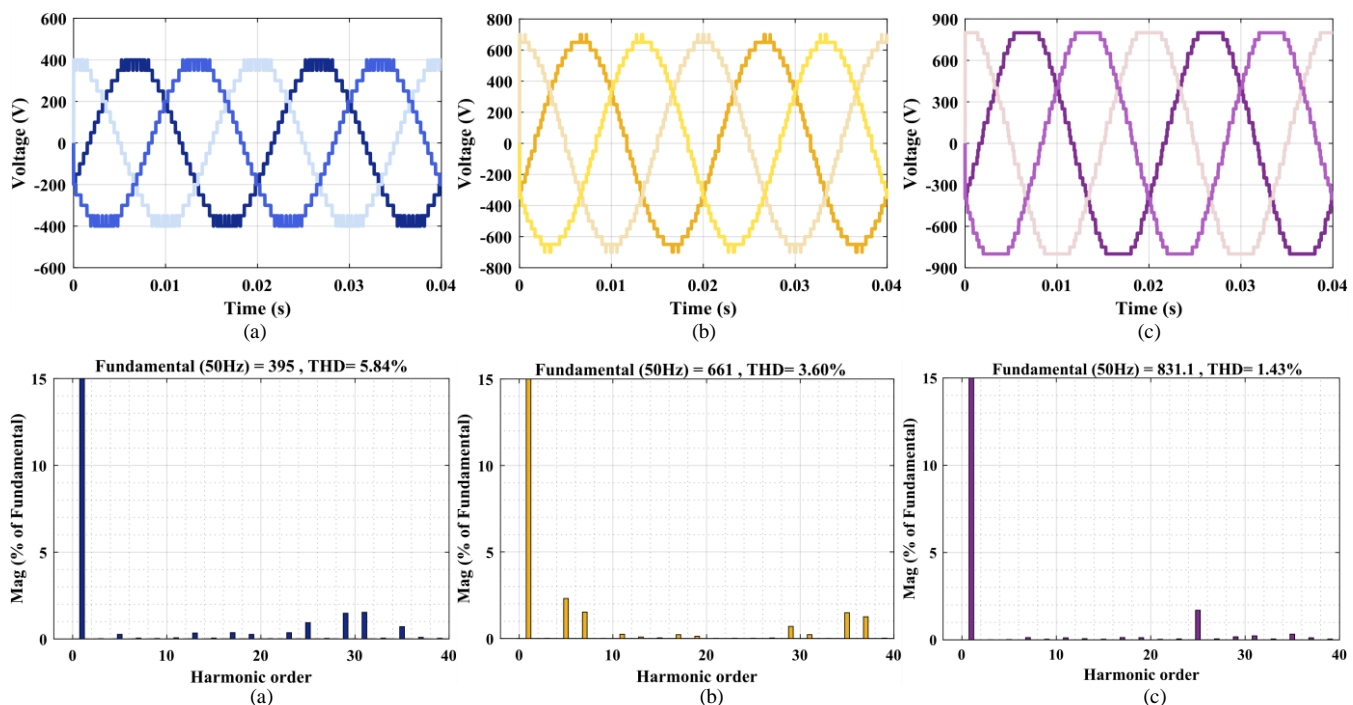
4

FIGURE 10. Simulation results of three-phase 17-level CHB MLI: (a) line voltages at *m* = 0.4, (b) line voltages at *m* = 0.7, (c) line voltages at *m* = 1, (d) THD of line voltage *ab* at *m* = 0.4, (e) THD of line voltage *ab* at *m* = 0.7, and (f) THD of line voltage *ab* at *m* = 1.

TABLE V
THD CALCULATION AND COMPARISON STUDY BETWEEN DIFFERENT OPTIMIZATION ALGORITHMS

Modulation index (*m*)	THD calculation using different algorithms (%)																	
	PSO [13]			WOA [14]			DHS [16]			GA [17]			IIA [18]			OQBA		
	1	2	3	1	2	3	1	2	3	1	2	3	1	2	3	1	2	3
0.1	40.48	38.88	21.03	40.48	38.08	21.17	41.31	34.38	30.94	57.95	31.71	29.33	40.48	29.07	22.49	40.12	27.03	14.37
0.2	38.38	32.93	9.64	38.77	18.65	9.64	32.72	34.38	18.99	33.03	21.05	12.42	39.25	18.51	10.25	30.45	15.37	7.95
0.3	33.37	19.60	7.93	29.47	17.19	8.14	25.74	8.64	7.86	28.88	9.74	7.90	27.30	17.15	8.42	17.76	7.90	6.67
0.4	33.37	8.49	7.93	29.47	17.19	8.14	25.74	8.64	7.86	24.79	8.64	7.40	16.17	9.93	6.32	13.11	6.47	5.87
0.5	22.21	8.49	7.93	29.47	7.27	7.66	11.60	7.20	6.45	11.87	7.20	5.68	11.27	7.42	5.67	9.74	5.97	4.95
0.6	22.21	8.49	7.93	29.47	5.60	6.12	11.60	6.60	5.57	10.85	5.55	5.13	11.27	7.42	4.26	7.68	5.35	4.20
0.7	22.21	6.65	5.89	29.47	4.90	5.57	10.13	6.47	4.88	9.65	5.04	4.30	11.27	5.23	4.00	6.41	4.62	3.60
0.8	22.21	6.65	5.89	29.47	4.25	3.37	6.59	5.63	3.73	7.94	4.39	3.83	11.27	4.61	4.00	5.64	4.05	2.03
0.9	22.21	5.24	5.89	29.47	4.25	3.37	6.59	4.42	3.73	7.55	4.24	3.22	11.27	4.61	4.00	5.29	2.86	1.64
1	22.21	5,24	5.89	29.47	4.25	3.37	6.59	4.42	3.73	6.17	4.07	2.87	11.27	4.61	4.00	5.08	2.70	1.43

WOA based SHEPWM was done for 11-level inverters and it shows comparatively better result than both PSO and DE for the case study 2. This indicates that these algorithms only perform slightly better when the optimizable variables or switching angles are increased. It also signifies that these algorithms are inoperative for low-level inverters which is a huge disadvantage. DHS performed much better in 1st case study compared to PSO, DE, and WOA. However, it also could not produce any solution at *m* > 0.8 and most of its generated THD did not follow IEEE 519 standard except at *m* ≥ 0.8. On the contrary, GA performed well and found solutions under all modulation indices similar to the proposed OQBA. Moreover, it produced THD following IEEE 519 only at *m* ≥ 0.8 which is similar to DHS. Therefore, for the 1st case study, it can be easily concluded that OQBA

outperformed all other algorithms since it was not only able to find solutions under all modulation indices but also generated output voltages having better harmonic profiles. The THDs generated by OQBA algorithm followed IEEE 519 standard at *m* ≥ 0.6.

In the 2nd case study, all algorithms performed significantly better. However, in this case study PSO again performed poorly compared to other algorithms. This is understandable since PSO is a 1st generation algorithm and a lot of improvements in swarm optimization have been made in recent years to enhance performance [34]. WOA and IIA generated similar set of results as reported in [14] and [18] respectively. WOA's performance became much better in this case study since this algorithm works better with higher optimization variables [14]. However, both WOA and IIA
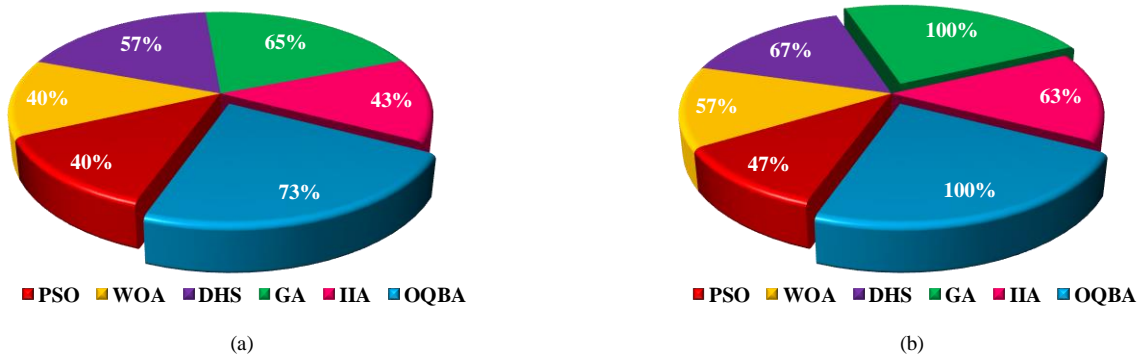
FIGURE 11. Performance of the optimization algorithms for: (a) 1st objective and, (b) 2nd objective.

could not find any solution at $m > 0.8$. It can be also validated from the results in [14] and [18]. DHS performed better in terms of finding solutions compared to both WOA and DE, but the harmonic profile was slightly poorer. The results shown in [16] was generated for a higher 27-level MLI which is why the harmonic profile was better. Nevertheless, for higher-level MLIs, the execution of SHEPWM becomes unnecessary as reported in [7]. MLIs capable of generating higher voltage levels generally produce better harmonic profile even with fundamental low-frequency modulation techniques such as nearest level control (NLC) and nearest space control (NPC). Besides, the results generated in [16] applied a very high number of iterations which have been avoided in this study due to its shortcomings. In this case study, the GA performed better than the other algorithms. Still, the proposed OQBA outperformed the other algorithms in this case study as it produced a better harmonic profile following IEEE 519 standard and global solutions under all modulation indices.

The final case study has demonstrated incremental improvements in terms of harmonic profile for all the algorithms. In this case, all algorithms have performed better and the generated THDs have followed IEEE 519 standard. This case study also implies that as the number of levels produced by the MLIs increases the performance benchmark of all the optimization algorithms become very similar and highly enhanced. Therefore, the advantages of a certain algorithm become a bit difficult to be justified by comparison. Yet, it can be clearly observed from the results of the 3rd case study that the proposed algorithm has produced better results and significantly reduced the THD at $m \geq 0.3$.

The entire comparative study was analyzed for a total of 30 results applying each optimization algorithm. The performance of all the algorithms is justified based on the two primary objectives of this study which are shown as graphical illustrations in Fig. 11(a) and Fig. 11(b), respectively. WOA and PSO performed the poorest in 1st objective while only PSO performed the poorest in the 2nd objective. On the contrary, it can be observed that for the 1st objective shown in Fig. 11(a), the proposed OQBA

performed the finest by producing 22 out of 30 results that have followed IEEE 519 standards. For the 2nd objective, both OQBA and GA have found solutions for all 30 cases which is depicted in Fig. 11(b).

The comparative analysis is extended by comparing the proposed algorithm with hybrid-PSO (HPSO) based SHEPWM implemented in two switched capacitor based MLIs [36], [37]. It should be addressed that the topological difference of MLIs will not have any impact on the THD. In other words, the 11-level inverter proposed in [36] will produce same THD as an 11-level CHB MLI provided that the optimization technique used for determining the switching angles is same for both MLIs. Besides, conducting comparative analysis between different MLI topology is not an objective of this manuscript. The switching angles provided in [36] for an 11-level CHB MLI has produced THD of 6.57% at $m = 0.8$ which is almost close to the THD of 6.65% for PSO as shown in Table V. OQBA has produced only 4.05% THD at $m = 0.8$ for an 11-level CHB MLI. The proposed algorithm is also compared with 2 other algorithms which are Flower Pollination Algorithm (FPA) [38], and Teaching Learning Based Optimization (TLBO) [39] for an 11-level CHB MLI. The results are shown in Table VI and it can be noticed that OQBA has produced less THD than these 3 algorithms for different modulation indices which shows

TABLE VI
EXTENSIVE COMPARATIVE STUDY WITH PSO

Algorithm	Voltage Level (N_L)	Modulation Index (m)	THD (%)
HPSO [36]	11	0.8	6.57
		0.6	6.10
FPA [38]	11	0.8	4.70
		1	5.10
		0.6	8.20
TLBO [39]	11	0.8	4.60
		1	8.00
		0.6	5.35
OQBA	11	0.8	4.05
		1	2.70
		0.3	31.47
AQPSO [40]	7	0.6	10.44
		0.8	7.17
		0.3	17.76
OQBA	7	0.6	7.68
		0.8	5.64

its superiority over these algorithms. A combinational optimization algorithm between conventional PSO and GA is proposed in [40], which is named as Asynchronous Particle Swarm Optimization Genetic Algorithm (APSOGA). The switching angles determined by APSOGA for a 7-level MLI has produced THD of 31.47%, 10.44% and 7.17% at $m = 0.3$, $m = 0.6$ and $m = 0.8$, respectively. At the same modulation indices, OQBA has produced THD of 17.76%, 7.68% and 5.64%. These results again prove the preeminence of the proposed algorithm.

VI. EXPERIMENTAL RESULTS

The results obtained through simulation is further verified in this section by conducting an experimental analysis. The experimental results were obtained by developing a hardware prototype as shown in Fig. 12. The proposed OQBA based SHEPWM is executed by using TMS320F28335 digital signal processor. A three-phase resistive-inductive load of $(253\Omega - 0.53H)$ is connected at the output. The CHB MLI's output voltage and load current are measured for all case studies. On the other hand, the THD is measured using Fluke 43B power analyser tool. The DC

source voltages for all CHB MLIs are adjusted to 50 V which is similar to the simulation model. The experimental results or the 1st case study (7-level CHB MLI) are shown in Fig. 13(a). In addition, the harmonic spectrum of the output voltage is shown in Fig. 13(d). The results are generated with modulation index, $m = 1$ and fundamental frequency, $f = 50$
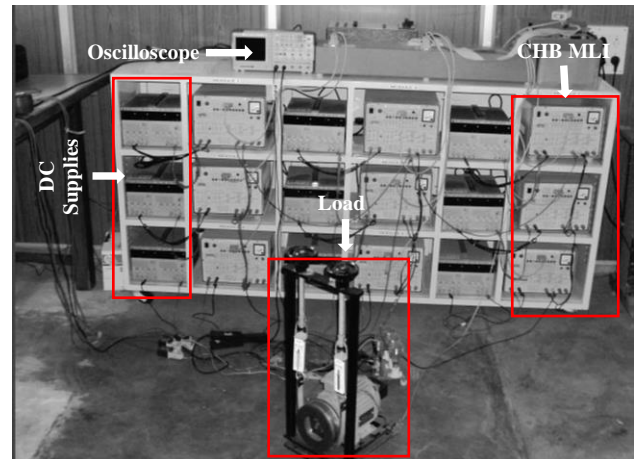

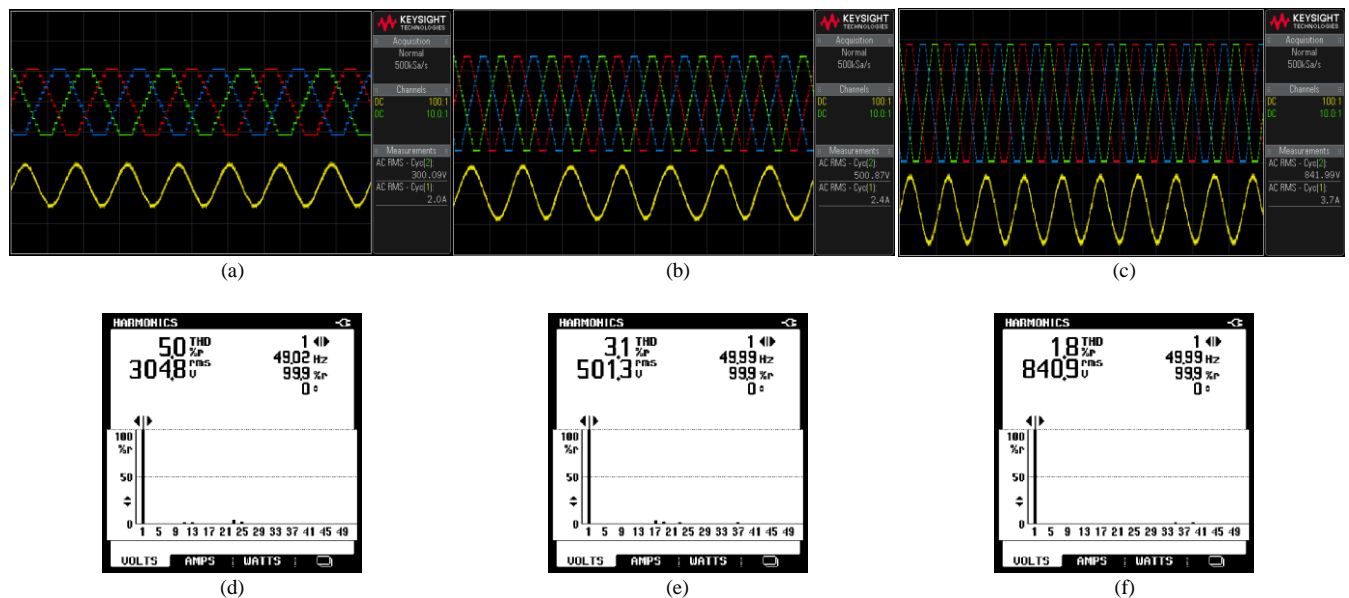**FIGURE 12.** Experimental setup for the three-phase CHB MLI.

FIGURE 13. Experimental results at $m = 1$ and $f = 50$ Hz for: (a) line voltages and current of 1st case study, (b) line voltages and current of 2nd case study, (c) line voltages and current of 3rd case study, (d) harmonic spectrum of 1st case study, (e) harmonic spectrum of 2nd case study, (f) harmonic spectrum of 3rd case study.

Hz. The output voltage is illustrated by yellow color while the load current is depicted by green color. The harmonic spectrum measured by the power quality analyzer is given for 50th harmonic order. It can be observed from the harmonic spectrum that the targeted 5th and 7th harmonics have been eliminated. Furthermore, the overall THD is 5% which is almost same as the simulation result and it is following IEEE 519 standard. Here, the most significant harmonic appeared to be 23rd and 25th. The triplen harmonics are also eliminated due to the implementation of a balanced

three-phase system. Although the frequency was low, the quality of the output voltage was maintained because of eliminating the lower-order harmonics.

The performance of the OQBA technique for the 2nd case study is shown in Fig. 12(b) and Fig. 12(e). The results, in this case, are also obtained for $m = 1$ and $f = 50$ Hz. In this case, the output voltage is increased to 250.77 V because of implementing 11-level CHB MLI. The THD of the output voltage has decreased from 5% to 3.07% as shown in Fig. 12 since four lower-order harmonics are removed. The highest

harmonics has emerged 17th and 19th for the 11-level CHB MLI. The results also showed high similarity with the obtained results in the simulation.

Finally, the performance of the OQBA based SHEPWM is analyzed for the 17-level CHB MLI. The output voltage along with the load current and the harmonic spectrum are shown in Fig 12(c) and Fig. 12(f), respectively for $m = 1$ and $f = 50$ Hz. It can be observed that the output voltage has increased to the maximum value of 400.87 V. Additionally, because of eliminating 7 lower-order harmonics, the overall THD in this case study has significantly decreased to only 1.8% which is well below the required IEEE 519 benchmark.

VII. PERFORMANCE ANALYSIS UNDER TRANSIENT CONDITIONS

The performance of the proposed algorithm is further justified in this section under two types of transient conditions: (i) sudden fluctuation of DC voltage and (ii) sudden fluctuation of the modulation index.

A. VOLTAGE FLUCTUATION

The performance analysis of OQBA under sudden fluctuation of DC voltage is conducted using MATLAB simulation. 7-level CHB MLI is considered for this analysis. The line voltage of the CHB MLI is shown in Fig. 14. It can be observed that the DC fluctuation is imposed on 0.5 sec. The DC voltage is varied from 50 V to 25 V and therefore, the line voltage has decreased from 300 V to 150 V. However, no other difference can be observed in the output voltage after the fluctuation. Furthermore, the harmonic spectrums of the line voltage before and after the fluctuation
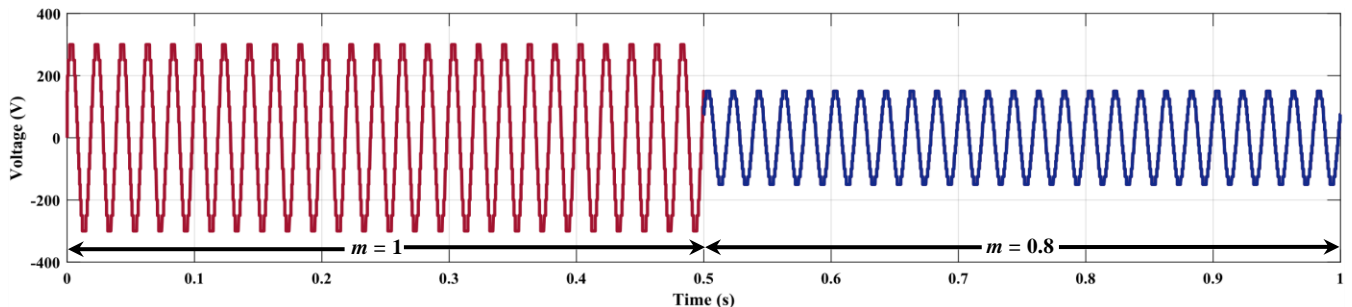
are shown in Fig. 15(a) and Fig. 15(b), respectively. It can be noticed that the voltage fluctuation did not alter the THD of the line voltage and it remained constant at 5.08%. This also verifies the consistent performance of OQBA under fluctuation in DC voltage.

A. FLUCTUATION IN MODULATION INDEX

To validate the performance of OQBA under variable modulation index, the three-phase 11-level CHB inverter of case study 2 is connected with a three-phase induction motor drive. The experimental analysis is performed by executing an open loop speed control technique of motor known as constant *V/f* technique [41]. The analysis is executed by running the induction motor at 3 different reference speeds regarded as 3 operating modes. The change of speed contributed to the change in the frequency and in the modulation index. At every operating mode, OQBA based SHEPWM is utilized to generate 3 sets of switching angles. The switching angles are already calculated and shoed in Table IV. The speed of the induction motor is varied from 450rpm → 900rpm → 1500rpm and therefore, the modulation index is also increased to 0.3→0.6→1. This range of modulation indices is selected to keep a similarity with the simulation results. It facilitated to verify whether the experimental results are accurate or not.

The transient line voltage and current of the 11-level CHB MLI is shown in Fig. 16. The harmonic spectrums of the 3 operating modes are shown in Fig. 17(a), Fig. 17(b) and Fig. 17(c), respectively. It can be observed that under the variable modulation index the THDs produced by the 11-level CHB

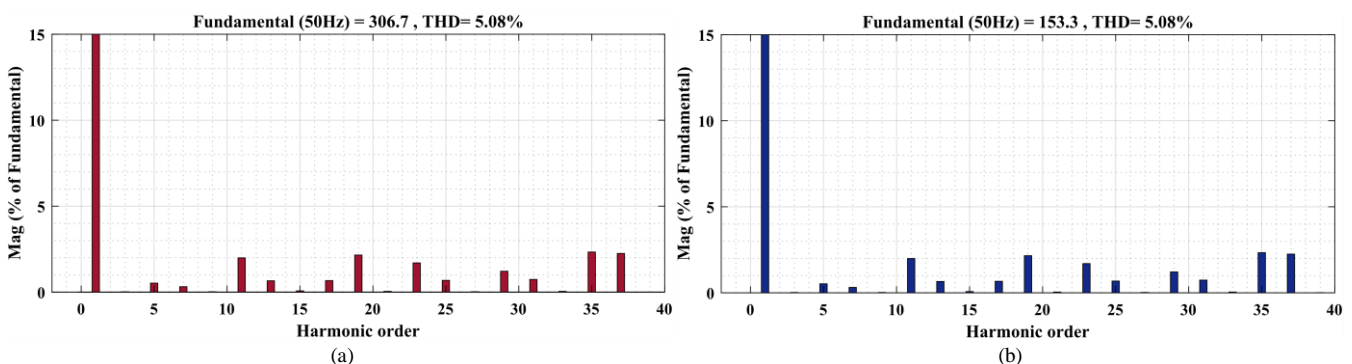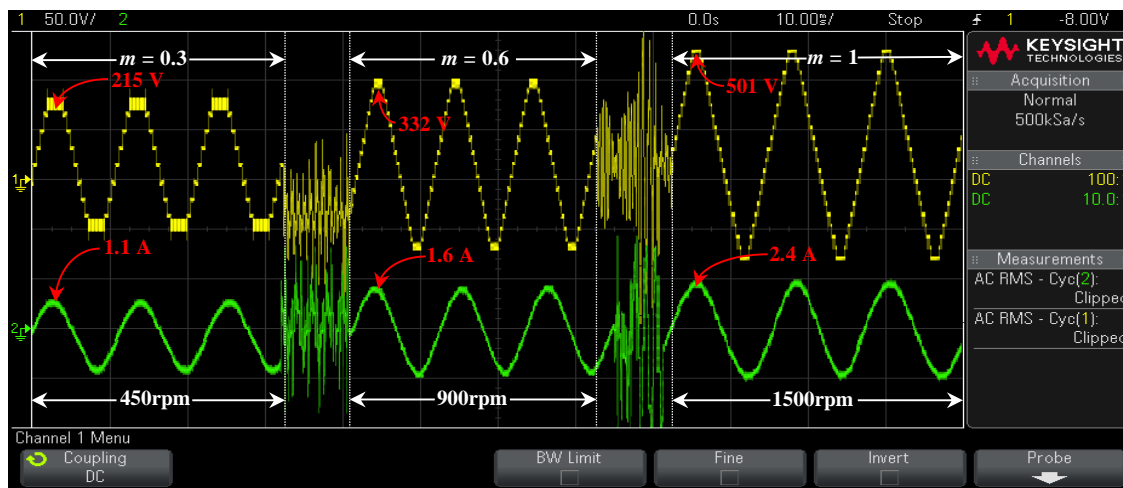**FIGURE 14.** Output voltage of 7-level CHB MLI under voltage fluctuation.

FIGURE 15. Harmonic spectrums of 7-level CHB MLI: (a) before voltage fluctuation (50 V), (b) after voltage fluctuation (25 V).

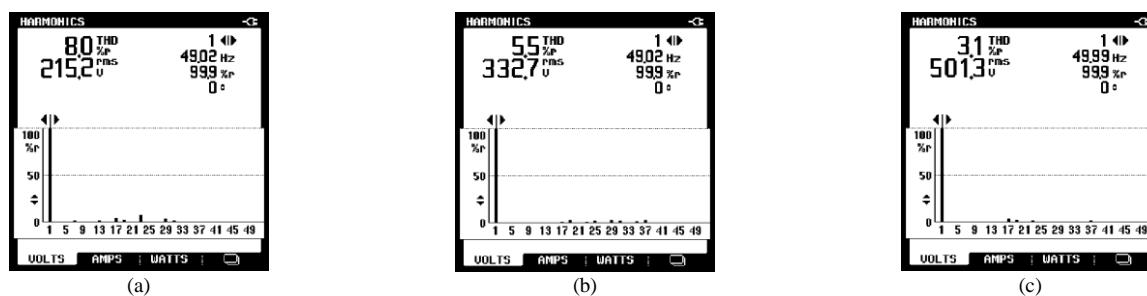**FIGURE 16. Output voltage of 11-level CHB MLI under fluctuation in modulation index.**

FIGURE 17. Harmonic spectrums of 11-level CHB MLI: (a) at $m = 0.3$, (b) $m = 0.6$, (c) $m = 1$.

MLI in each operation mode are almost reminiscent of the THDs produced in the simulation results which validates the accuracy of this analysis. Some small noises can be observed in the output which is due to the transition of switching angles keyed in by OQBA. Thus, it can be concluded that the proposed OQBA has performed without any issue under the sudden fluctuation in the modulation index.

VIII. FITNESS VALUE ANALYSIS

In this particular application of optimization algorithms, different modulation indices will create different convergence curves. Hence, the objective fitness value versus modulation index is plotted in Fig. 18. It can be

observed that the minimum objective fitness value is obtained by the OQBA technique for different modulation indices compare to all other optimization algorithms. The solutions (switching angels) of (27) that provide minimum fitness value have provided minimum THD in the output voltage. Fig.18 shows that for almost all modulation indices the minimum objective value is achieved by the proposed OQBA technique. In each case study, the OQBA technique provided better fitness value. Hence, the switching angels which provided minimum fitness value in the OQBA technique have decreased the THD of the output voltage. The convergence curves under different number of iterations are
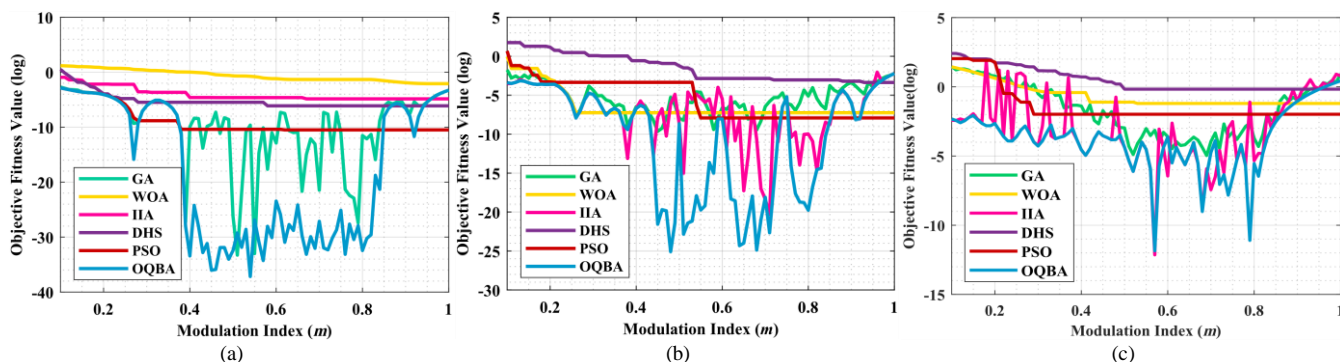

FIGURE 18. Fitness value of the optimization algorithms under different modulation indices: (a) 1st case study, (b) 2nd case study, (c) 3rd case study.
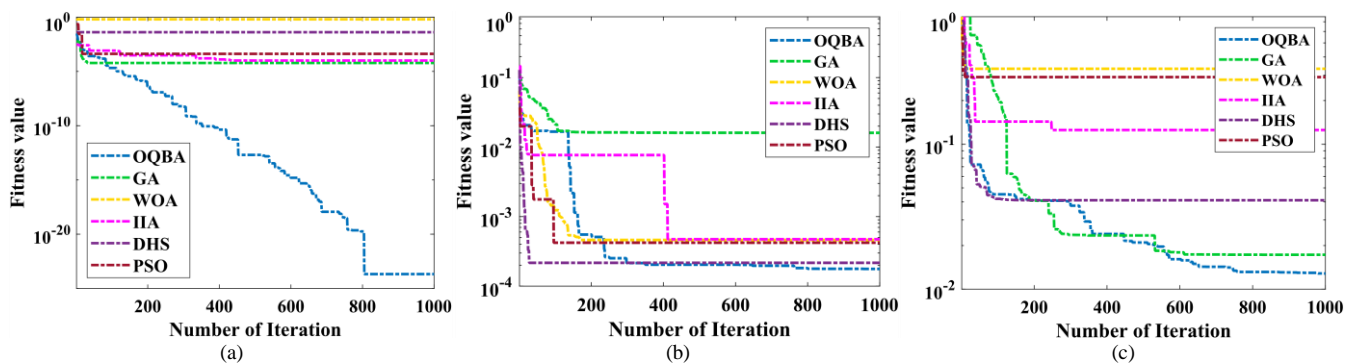
FIGURE 19. Convergence curves of the optimization algorithms: (a) 1st case study, (b) 2nd case study, (c) 3rd case study.
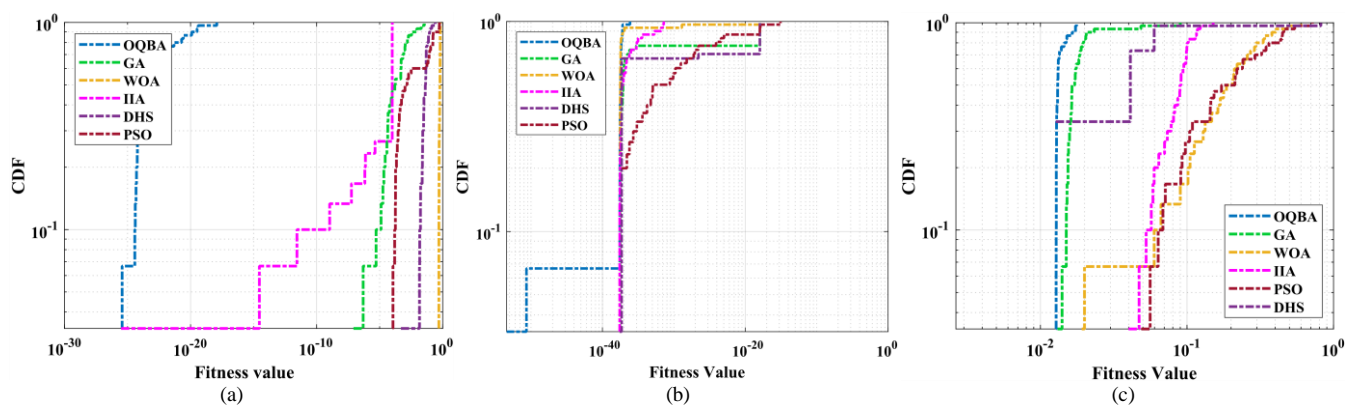

FIGURE 20. Convergence distribution function of the optimization algorithms: (a) 1st case study, (b) 2nd case study, (c) 3rd case study.
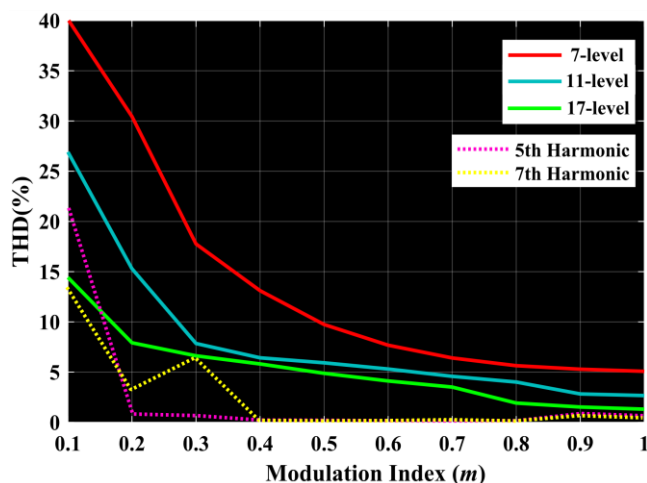

FIGURE 21. THD generated by OQBA under different modulation indices.

plotted in Fig. 19. It can be observed that under all case studies the minimum objective value is achieved by the proposed OQBA technique compared to all other algorithms.

The cumulative distribution function (CDF) of the obtained solutions for different algorithms are shown in Fig. 20. It can be observed from Fig. 20 that the proposed algorithm has clearly obtained high probability of

convergency for the 1st case study. For the 2nd and 3rd case studies, although OQBA achieved comparatively better convergence probability, the results are very close. This proves the previous statement that as the number of optimization variables increase, the performance of the algorithms become similar.

Finally, the THD of 3 different case studies generated by OQBA under different modulation studies are shown in Fig. 21. In addition, the 5th and 7th order harmonics for 1st case study under different modulation indices are also shown. It can be noticed that OQBA has kept these harmonics to almost zero in the range of $0.4 \leq m \leq 1$. It also verifies the superior optimization quality and the accuracy of the algorithm.

IX. CONCLUSION

The opposition-based quantum bat algorithm (OQBA) is proposed to optimize switching angles and eliminate selective harmonics of multilevel inverters. The performance of the proposed algorithm was verified by both simulation and DSP-based experimental prototype. This algorithm effectively overcomes most of the drawbacks hold by the other metaheuristic algorithms as well as mathematical strategies applied for SHEPWM. Three separate case studies verified that OQBA successfully accomplished two predefined objectives and outperformed other recently

proposed algorithms. It also verified that the proposed strategy is applicable for any multilevel inverter topology. Statistical analysis is also conducted to show that the performance of the proposed algorithm stays almost same even with multiple iterations and run times. The performance of the proposed algorithm is also analyzed under transient conditions and it performed excellently. The simulation and experimental results showed that in 73% of the total data, OQBA successfully kept the THD of the output voltage below the permissible THD set by IEEE 519 standard. Therefore, it can be concluded that OQBA can enhance the performance of any multilevel inverter topology and can be a real candidate to replace other available modulation strategies in industrial applications. The main concluding remarks are as follows:

- Quantum bat algorithm is incorporated with oppositional-based learning to avoid local optima and premature convergence.
- Comparative analysis shows that the standalone search algorithms cannot perform well.
- In each case study, the OQBA technique provided better fitness value.

REFERENCES

[1] M. S. A. Dahidah, G. Konstantinou, and V. G. Agelidis, "A Review of Multilevel Selective Harmonic Elimination PWM: Formulations, Solving Algorithms, Implementation and Applications," *IEEE Trans. Power Electron.*, vol. 30, no. 8, pp. 4091–4106, 2015.

[2] V. G. Agelidis, A. Balouktsis, I. Balouktsis, and C. Cossar, "Multiple sets of solutions for harmonic elimination PWM bipolar waveforms: Analysis and experimental verification," *IEEE Trans. Power Electron.*, vol. 21, no. 2, pp. 415–421, 2006.

[3] M. Srndovic, A. Zhetessov, T. Alizadeh, Y. L. Familiant, G. Grandi, and A. Ruderman, "Simultaneous Selective Harmonic Elimination and THD Minimization for a Single-Phase Multilevel Inverter with Staircase Modulation," *IEEE Trans. Ind. Appl.*, vol. 54, no. 2, pp. 1532–1541, 2018.

[4] S. Kundu, A. D. Burman, S. K. Giri, S. Mukherjee, and S. Banerjee, "Comparative study between different optimisation techniques for finding precise switching angle for SHE-PWM of three-phase seven-level cascaded H-bridge inverter," *IET Power Electron.*, vol. 11, no. 3, pp. 600–609, Mar. 2018.

[5] S. T. Meraj, A. Ahmed, L. K. Haw, A. Arif, and A. Masaoud, "DSP Based Implementation of SHE-PWM for Cross-Switched Multilevel Inverter," in *Proceedings - 2019 IEEE 15th International Colloquium on Signal Processing and its Applications, CSPA 2019*, Apr. 2019, pp. 54–59.

[6] M. Al-Hitmi, S. Ahmad, A. Iqbal, S. Padmanaban, and I. Ashraf, "Selective harmonic elimination in a wide modulation range using modified Newton-raphson and pattern generation methods for a multilevel inverter," *Energies*, vol. 11, no. 2, 2018.

[7] S. T. Meraj, N. Z. Yahaya, K. Hasan, and A. Masaoud, "A hybrid T-type (HT-type) multilevel inverter with reduced components," *Ain Shams Eng. J.*, vol. 12, no. 2, pp. 1959–1971, Feb. 2021.

[8] J. N. Chiasson, L. M. Tolbert, K. J. McKenzie, and Z. Du, "Control of a multilevel converter using resultant theory," *IEEE Trans. Control Syst. Technol.*, vol. 11, no. 3, pp. 345–354, May 2003.

[9] A. Moeini, H. Zhao, and S. Wang, "A Current-Reference-Based Selective Harmonic Current Mitigation PWM Technique to Improve the Performance of Cascaded H-Bridge Multilevel Active Rectifiers," *IEEE Trans. Ind. Electron.*, vol. 65, no. 1, pp. 727–737, Jan. 2018.

[10] S. Li, G. Song, M. Ye, W. Ren, and Q. Wei, "Multiband SHEPWM Control Technology Based on Walsh Functions," *Electronics*, vol. 9, no. 6, p. 1000, Jun. 2020.

[11] M. Vadizadeh, "Improved SHEPWM Strategy By The Robustness Optimization Algorithm In Multilevel Inverters With Equal DC Sources," *IOSR J. Electr. Electron. Eng.*, vol. 9, no. 4, pp. 80–88, 2014.

[12] S. A. Kandil, A. A. Ali, A. El Samahy, S. M. Wasfi, and O. P. Malik, "Harmonic optimization in voltage source inverter for PV application using heuristic algorithms," *Int. J. Emerg. Electr. Power Syst.*, vol. 17, no. 6, pp. 671–682, Dec. 2016.

[13] R. N. Ray, D. Chatterjee, and S. K. Goswami, "An application of PSO technique for harmonic elimination in a PWM inverter," *Appl. Soft Comput. J.*, vol. 9, no. 4, pp. 1315–1320, Sep. 2009.

[14] S. Kumar Dash, B. Nayak, and J. Ballav Sahu, "Selective Harmonic Elimination of an Eleven Level Inverter Using Whale Optimization Technique," *Int. J. Power Electron. Drive Syst.*, vol. 9, no. 4, p. 1944, 2018.

[15] A. Hiendro, "Multiple switching patterns for SHEPWM inverters using differential evolution algorithms," *Int. J. Power Electron. Drive Syst.*, vol. 1, no. 2, pp. 94–103, Sep. 2011.

[16] Y. Xin, J. Yi, K. Zhang, C. Chen, and J. Xiong, "Offline Selective Harmonic Elimination with (2N+1) Output Voltage Levels in Modular Multilevel Converter Using a Differential Harmony Search Algorithm," *IEEE Access*, vol. 8, pp. 121596–121610, 2020.

[17] S. S. Lee, B. Chu, N. R. N. Idris, H. H. Goh, and Y. E. Heng, "Switched-Battery Boost-Multilevel Inverter with GA Optimized SHEPWM for Standalone Application," *IEEE Trans. Ind. Electron.*, vol. 63, no. 4, pp. 2133–2142, Apr. 2016.

[18] L. Sheng, S. Q. Qian, Y. Q. Ye, and Y. H. Wu, "An improved immune algorithm for optimizing the pulse width modulation control sequence of inverters," *Eng. Optim.*, vol. 49, no. 9, pp. 1463–1482, Sep. 2017.

[19] T. Sudhakar Babu, K. Priya, D. Maheswaran, K. Sathish Kumar, and N. Rajasekar, "Selective voltage harmonic elimination in PWM inverter using bacterial foraging algorithm," *Swarm Evol. Comput.*, vol. 20, pp. 74–81, Feb. 2015.

[20] E. Deniz, O. Aydogmus, and Z. Aydogmus, "Implementation of ANN-based Selective Harmonic Elimination PWM using Hybrid Genetic Algorithm-based optimization," *Meas. J. Int. Meas. Confed.*, vol. 85, pp. 32–42, May 2016.

[21] F. Chabni, R. Taleb, and M. Helaimi, "Optimum SHEPWM for a new 21-level inverter topology using numerical optimization methods: experimental comparative study," *J. Vib. Control*, vol. 24, no. 23, pp. 5556–5569, Dec. 2018.

[22] T. M. Hossain, J. Watada, I. A. Aziz, and M. Hermana, "Machine Learning in Electrofacies Classification and Subsurface Lithology Interpretation: A Rough Set Theory Approach," *Appl. Sci.*, vol. 10, no. 17, p. 5940, Aug. 2020.

[23] T. M. Hossain, J. Watada, I. A. Aziz, M. Hermana, S. T. Meraj, and H. Sakai, "Lithology prediction using well logs: A granular computing approach," *Int. J. Innov. Comput. Inf. Control*, vol. 17, no. 1, pp. 225–244, 2021.

[24] P. Vasant, F. P. Mahdi, J. A. Marmolejo-Saucedo, I. Litvinchev, R. R. Aguilar, and J. Watada, "Quantum-Behaved Bat Algorithm for Solving the Economic Load Dispatch Problem Considering a Valve-Point Effect," *Int. J. Appl. Metaheuristic Comput.*, vol. 11, no. 3, pp. 41–57, Mar. 2020.

[25] A. Jamasb, S.-H. Motavalli-Anbaran, and H. Zeyen, "Non-linear stochastic inversion of gravity data via quantum-behaved particle swarm optimisation: application to Eurasia-Arabia collision zone (Zagros, Iran)," *Geophys. Prospect.*, vol. 65, pp. 274–294, Dec. 2017.

[26] J. Islam, S. T. Meraj, B. Negash, and K. Biswas, "Modified Quantum Particle Swarm Optimization For Selective Harmonic Elimination (SHE) in A Single-phase Multilevel Inverter," *Int. J. Innov. Comput. Inf. Control*, vol. 17, no. 3, pp. 959–971, 2021.

[27] O. H. Montiel Ross, "A Review of Quantum-Inspired Metaheuristics: Going from Classical Computers to Real Quantum Computers," *IEEE Access*, vol. 8, pp. 814–838, 2020.

[28] B. Zhu, W. Zhu, Z. Liu, Q. Duan, and L. Cao, "A Novel Quantum-Behaved Bat Algorithm with Mean Best Position Directed for Numerical Optimization," *Comput. Intell. Neurosci.*, vol. 2016, 2016.

[29] J. Islam, B. Mamo Negash, P. Vasant, N. Ishtiaque Hossain, and J. Watada, "Quantum-Based Analytical Techniques on the Tackling of Well Placement Optimization," *Appl. Sci.*, vol. 10, no. 19, p. 7000, Oct. 2020.

[30] H. R. Tizhoosh, "Opposition-based learning: A new scheme for

machine intelligence," in *Proceedings - International Conference on Computational Intelligence for Modelling, Control and Automation, CIMCA 2005 and International Conference on Intelligent Agents, Web Technologies and Internet*, 2005, vol. 1, pp. 695–701.

[31] P. K. Roy, C. Paul, and S. Sultana, "Oppositional teaching learning based optimization approach for combined heat and power dispatch," *Int. J. Electr. Power Energy Syst.*, vol. 57, pp. 392–403, May 2014.

[32] P. K. Roy and D. Mandal, "Oppositional biogeography-based optimisation for optimal power flow," *Int. J. Power Energy Convers.*, vol. 5, no. 1, pp. 47–69, 2014.

[33] S. T. Meraj *et al.*, "A Diamond Shaped Multilevel Inverter with Dual Mode of Operation," *IEEE Access*, vol. 9, pp. 59873–59887, 2021.

[34] M. Li, W. Du, and F. Nian, "An adaptive particle swarm optimization algorithm based on directed weighted complex network," *Math. Probl. Eng.*, vol. 2014, 2014.

[35] T. Eltaeib and A. Mahmood, "Differential Evolution: A Survey and Analysis," *Appl. Sci.*, vol. 8, no. 10, p. 1945, Oct. 2018.

[36] M. D. Siddique, S. Mekhilef, N. M. Shah, and M. A. Memon, "Optimal Design of a New Cascaded Multilevel Inverter Topology With Reduced Switch Count," *IEEE Access*, vol. 7, pp. 24498–24510, 2019.

[37] M. D. Siddique, A. Iqbal, M. A. Memon, and S. Mekhilef, "A new configurable topology for multilevel inverter with reduced switching components," *IEEE Access*, vol. 8, pp. 188726–188741, 2020.

[38] K. P. Panda, P. R. Bana, and G. Panda, "FPA Optimized Selective Harmonic Elimination in Symmetric-Asymmetric Reduced Switch Cascaded Multilevel Inverter," in *IEEE Transactions on Industry Applications*, May 2020, vol. 56, no. 3, pp. 2862–2870.

[39] S. Muralidharan, J. Gnanavadivel, M. Y. S. Muhaidheen, and S. Menaka, "Harmonic elimination in multilevel inverter using TLBO algorithm for marine propulsion system," *Mar. Technol. Soc. J.*, vol. 55, no. 2, pp. 117–126, Mar. 2021.

[40] M. A. Memon, M. D. Siddique, M. Saad, and M. Mubin, "Asynchronous Particle Swarm Optimization-Genetic Algorithm (APSO-GA) based Selective Harmonic Elimination in a Cascaded H-Bridge Multilevel Inverter," *IEEE Trans. Ind. Electron.*, 2021.

[41] S. T. Meraj, K. Hasan, and A. Masaoud, "Design and application of SPWM based 21-level hybrid inverter for induction motor drive," *TURKISH J. Electr. Eng. Comput. Sci.*, vol. 28, no. 6, pp. 3219–3234, Nov. 2020.